

T H E U N I V E R S I T Y O F M I C H I G A N  
COLLEGE OF ENGINEERING  
Department of Meteorology and Oceanography

TURBULENCE MEASUREMENTS MADE FROM FLIP IN BOMEX

Third Annual Report of

An Investigation of the Structure of Turbulence  
and of the Turbulent Fluxes of Momentum and Heat Over Water Wave

For the Period: 15 August 1969 to 15 August 1970

Donald J. Portman  
Kenneth L. Davidson  
Michael A. Walter

ORA Project 08849

under contract with:

OFFICE OF NAVAL RESEARCH  
DEPARTMENT OF THE NAVY  
CONTRACT NO. N00014-67-A-0181-0005, PROJECT NO. NR-083-224  
WASHINGTON, D.C.

administered through:

OFFICE OF RESEARCH ADMINISTRATION      ANN ARBOR

August 1970

Distribution of this document is unlimited.

## ABSTRACT

Simultaneous measurements of wind velocity components with hot-film anemometers, air temperature fluctuations, and wave heights were made about 200 miles east northeast of Barbados during BOMEX. A total of 54 hours of measurements were made during the last two weeks in May, 1969. Of these, 23 had simultaneous recordings of wind velocity components and temperature fluctuations at two heights. Measurement heights were 2, 3, 6 and 8 meters above mean water level.

Three different computer facilities have been employed in processing the data to obtain probability distribution functions, joint probability distribution functions, spectrum functions and cross-spectrum functions for velocity components, temperature fluctuations and wave heights. Examples of the calculation results are given and briefly described. They show specific effects of waves on the velocity components.

## TABLE OF CONTENTS

	<u>Page</u>
ABSTRACT	ii
LIST OF TABLES	iv
LIST OF FIGURES	v
I INTRODUCTION	1
II SUMMARY OF MEASUREMENTS	5
III EQUIPMENT AND PROCEDURES	11
IV DATA PROCESSING PROCEDURES	22
V FIRST RESULTS	30
REFERENCES	39

## LIST OF TABLES

Table	<u>Page</u>
1. Dates, times and heights of measurements.	7-8
2. Sample turbulence statistics.	31

## LIST OF FIGURES

Figure	<u>Page</u>
1. Measurements and wind and wave conditions.	6
2. Three-sensor hot-film probe.	12
3. Hot-film sensor after use in BOMEX.	15
4. Sensor locations on FLIP.	17
5. Sensor mounting arrangement on FLIP.	19
6. Schematic of recording system components.	21
7. Data processing, stage 1.	23
8. Data processing, stage 2.	24
9. Non-dimensional ratios $\sigma_u/u_*$ , $\sigma_v/u_*$ , and $\sigma_w/u_*$ in relation to $z/L$ .	32
10. Non-dimensional ratio $\sigma_T/T_*$ in relation to $z/L$ .	33
11. Spectral results for 19 May 1969.	34
12. Phase relationships among velocity components and components of dominant surface wave, 19 May 1969.	36
13. Joint probability distributions among velocity components and dominant surface wave, 19 May 1969.	38

## I INTRODUCTION

During the last two weeks of May, 1969, University of Michigan personnel made a series of turbulence and wave measurements in the Barbados Oceanographic and Meteorological Experiment (BOMEX). The measurements were made about 200 miles east northeast of Barbados (in the vicinity of  $14^{\circ}\text{N}$  latitude,  $57^{\circ}\text{W}$  longitude) with instruments supported by the Scripps Institution of Oceanography Floating Instrument Platform (FLIP). They consisted of simultaneous recordings of wind velocity components (with hot-film anemometers), air temperature fluctuations and wave heights. There were about 54 hours of recordings in 40 separate observation periods; for about half of these, wind components and temperatures were measured simultaneously at two heights. The heights ranged from 2 to 8 m and the sensors and recording systems were capable of measuring velocity and temperature fluctuations at frequencies up to 50 Hz. All data were recorded synchronously with two 7-channel magnetic tape recorders.

The experiment had two purposes. First, it was desired to make direct measurements of the vertical turbulent fluxes of momentum and sensible heat to provide information for the BOMEX core experiment. The core experiment consists of analyses of the energy budget of an atmospheric volume 500 km on a side and about 5 km high and the heat budget of the upper part of the ocean underneath it.

The second purpose was a more general one but, also, has dir-

ect significance for BOMEX. It was simply to study the nature of airflow adjacent to ocean waves and, especially, the influence of waves on the turbulent flow over them. Of special interest in this regard is the relationship between vertical fluxes of momentum and heat and the vertical profiles of horizontal velocity and temperature. The profiles are the hoped-for link with which fluxes may be estimated from knowledge of the horizontal distributions of waves, water surface temperature, wind, and air temperature<sup>1</sup>. A number of investigators have reported, however, that flux-profile relationships that have been found useful for modeling and analyzing atmospheric dynamics over land have failed when applied to the air layer over waves. Kitaygorodskiy (1969) found, for example, that direct measurements of momentum flux (with an acoustic anemometer) were a factor of 2 to 4 greater than those determined from the wind profile in the way commonly applied to land measurements. The implication is that wind profiles over water are influenced by waves and until the nature of the influence is described and explained, flux estimates from profiles may not be possible.

The detailed nature of airflow over waves has been the subject of a number of theoretical and experimental investigations over the last dozen years. Theoretical studies (e.g., Miles, 1957, 1959; and Phillips, 1966) and most laboratory investigations (e.g., Karaki and Hsu, 1968; Stewart, 1968; Shemdin, 1969) have

---

<sup>1</sup>Wind and temperature profiles were measured from FLIP by C. W. Thornthwaite Associates at the same time that University of Michigan measurements were made. The results have already been reported by Superior (1969).

focused mainly on the questions of the initiation and growth of waves as they gain momentum from the airflow. On the other hand, Harris (1966) in a laboratory investigation, Yefimov and Sizov (1969) in an investigation in the Atlantic Ocean, and Davidson (1970) in measurements over waves in Lake Michigan have identified significant features in the airflow due to the wave motion below it.

To study the different aspects of the wind-wave coupling, it is convenient to identify the "critical level" (Miles, 1957), i.e., the height at which the mean wind speed equals the phase speed of the wave component corresponding to the wave spectrum peak. According to Miles' theory, the transfer of energy from wind to the waves is related to the wave-induced fluctuations in the airflow at the critical level. Phillips (1966) estimates that the momentum flux to the long waves by this mechanism is on the order of 10% of the total momentum transfer to the water surface.

When the phase speed of the wave component represented by the spectrum peak is large (so that the critical level is well above the surface), the influence of the waves on the airflow is, perhaps, a more important part of the wind-wave coupling phenomenon. From the works of Harris (1966), Yefimov and Sizov (1969), and of Davidson (1970) it is clear that waves can and do impart energy to the wind. It is clear, furthermore, that the effects will appear in the wind profile. The extent of the influence for different wind and wave conditions is yet to be determined, as is the meaning for flux-profile relationships.



The measurements reported here, when finally analyzed, should provide some insight on these matters. For two observation periods (both consisting of measurements made at 6 and 2 m above the mean water level), wind and wave spectra have been computed. The wave phase speeds corresponding to wave spectra peaks were nearly identical, viz., 15 and 16 m sec<sup>-1</sup>, as were the wind speeds (10 m sec<sup>-1</sup> at the 6-m level). The critical levels for these two periods were about 10 m. However, the significant wave heights in one period were 3 m and in the other 1 m. Unique measurements such as these, beneath the critical height, when fully analyzed should tell much about the momentum exchange and its relation to the wind profile.

At this time only part of the data for the two periods just mentioned has been analyzed. First results are described in the last section of this report. The remainder of the report is devoted to a description of the information recorded during the two week experiment, the equipment and procedures, and methods of data processing. This report should be regarded, therefore, as the first of a two part description of the findings of a short BOMEX experiment on turbulence over ocean waves.

## II SUMMARY OF MEASUREMENTS

Turbulence and supporting data were recorded for a total of 54 hours in 40 separate recording periods on eight days. Figure 1 shows measurement times and heights, visual wave height estimates and 10-m wind speeds determined from wind profiles. In this figure wave heights are shown as crest heights above mean water level. As can be seen they were estimated to be about 1 m most of the time with, however, an increase to about 2 m on May 28. The 10-m wind speed was generally between 7 and 10 m sec<sup>-1</sup> for the observation periods.

A list of measurement dates, times and heights is given in Table 1. About 58 per cent of the measurements were made between 0600 and 1800 local standard time. Of the 54 hours recorded, 23 were accomplished with wind velocity components and temperature fluctuation measurements made simultaneously at two heights. The two heights were generally either 3 and 8 m (719 minutes of recording) or 2 and 6 m (538 minutes). Fewer measurements were made simultaneously at 3 and 6 m (251 minutes) and there were only 33 minutes recorded for measurements at 2 and 8 m. When measurements were made at only one height, they were made at 8 m. Waves were measured during all measurement periods.

Wind and temperature profiles and wet bulb temperatures for the listed observation periods were measured by C. W. Thornthwaite Associates personnel. In Table 1, periods during which wind profile data are reported by Superior (1969) (or logged by University

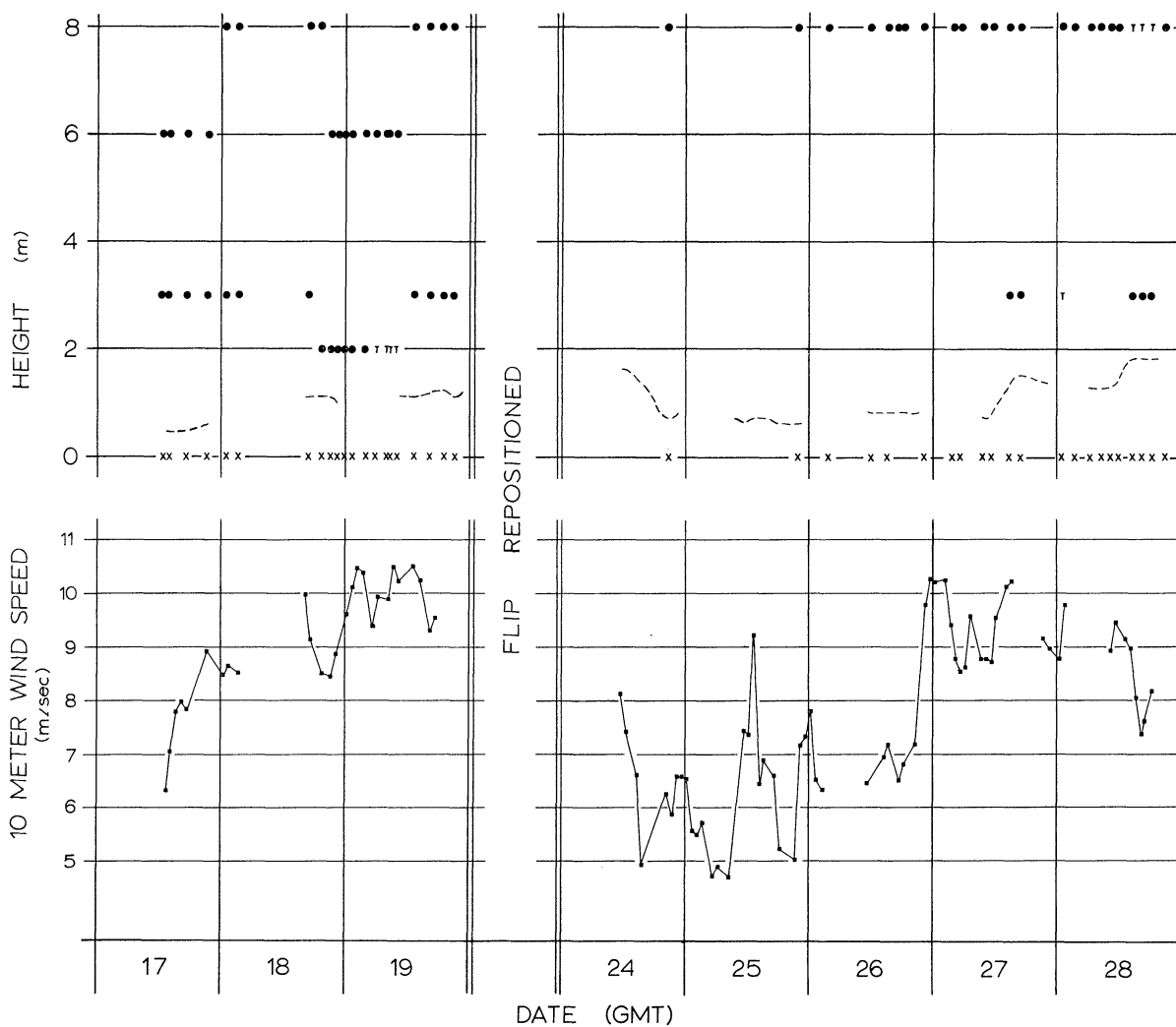


Figure 1. Measurements and wind and wave conditions.  
Upper half: The symbols and letters show heights and times of University of Michigan measurements aboard FLIP.

- -  $u'$ ,  $v'$ ,  $w'$ ,  $T'$
- T -  $T'$  only
- X - waves
- - visual estimates of wave heights

Lower half: Average wind speed at 10 meters.

Table 1

## Dates, Times and Heights of Measurements

Wind velocity components and temperatures were measured simultaneously at heights indicated. Waves were measured for all periods. Existence of C.W. Thornthwaite Associates profile data is shown in "CWT" column: wind profile data ( $\bar{U}$ ), wind profile data as read by University of Michigan personnel ( $\bar{U}_m$ ), and temperature profile data ( $\bar{T}$ ).

Date May, 1969	Time GMT	Record length minutes	Height meters	CWT
17	1232-1257	25	6 , 3	
	1324-1420	56	6 , 3	$\bar{U}$
	1655-1821	86	6 , 3	$\bar{U}$
	2112-2236	84	6 , 3	$\bar{U}$
18	0023-0145	82	8 , 3	$\bar{U}$
	0306-0425	79	8 , 3	$\bar{U}$
	1617-1740	83	8 , 3	$\bar{U}$
	1919-1952	33	8 , 2	$\bar{U}$
	2056-2142	46	6 , 2	$\bar{U}$
	2245-2256	11	6 , 2	
	2305-0020	75	6 , 2	
19	0057-0220	83	6 , 2	$\bar{U}$
	0308-0429	81	6 , 2	$\bar{U}$
	0546-0718	82	6 , 2	$\bar{U}$
	0754-0849	55	6 , 2*	$\bar{U}$
	0858-0921	23	6 , 2*	$\bar{U}$
	0945-1107	82	6 , 2*	$\bar{U}$
	1338-1450	72	8 , 3	$\bar{U}$
	1613-1735	82	8 , 3	$\bar{U}$
	1843-2003	81	8 , 3	$\bar{U}$
	2108-2223	75	8 , 3	$\bar{U}$
24	2020-2125	65	8	$\bar{U}$
25	2119-2242	83	8	$\bar{U}$
26	0327-0448	81	8	

\*Only temperature measurements made at this height.

Table 1 (continued)

Date May, 1969	Time GMT	Record length minutes	Height meters	CWT
26	1127-1211	44	8	$\bar{U}, \bar{T}$
	1431-1553	82	8	$\bar{U}, \bar{T}$
	1703-1742	39	8	$\bar{U}, \bar{T}$
	1759-1841	42	8	$\bar{U}, \bar{T}$
	2132-2252	83	8	$\bar{U}$
27	0311-0435	84	8	$\bar{U}$
	0458-0554	56	8	$\bar{U}$
	0901-1023	82	8	$\bar{U}$
	1058-1220	82	8	$\bar{U}$
	1419-1542	83	8, 3	$\bar{U}$
	1616-1738	82	8, 3	$\bar{U}_m$
28	0033-0155	82	8, 3*	$\bar{U}$
	0240-0403	83	8	$\bar{U}_m$
	0548-0714	86	8	$\bar{U}_m$
	0740-0902	82	8	$\bar{U}_m$
	0934-1055	81	8	$\bar{U}$
	1118-1220	62	8	$\bar{U}$
	1340-1502	82	8*, 3	$\bar{U}$
	1550-1712	82	8*, 3	$\bar{U}$
	1754-1916	82	8*, 3	$\bar{U}$
	2028-2150	82	8	$\bar{U}_m$

\*Only temperature measurements made at this height.

of Michigan investigators<sup>1</sup>) are indicated by " $\bar{U}$ " (or " $\bar{U}_m$ ") and temperature profile data by " $\bar{T}$ ". The wind profiles reported by Superior are given in 55-minute average speeds at heights of 2, 3, 4, 6, 8, 12 and 16 m, except for a few missing data. (The length of averaging time for other wind profiles varies from 5 to 20 minutes.) They were measured with matched, 3-cup anemometers whose starting speeds are reported to be about  $9 \text{ cm sec}^{-1}$  and distance constants about 83 cm.

Air temperatures are also given in 55-minute averages and there are data for heights of 2, 3, 4, 8 and 12 m. There are a few 16-m data on 26 May but 3-m data are missing for 26 and 27 May. The sensors were linearized thermistors, encased in glass beads, about 0.156 inches in diameter and supported in flat plate radiation shields.

The wind and temperature profile data are necessary for complete interpretation of turbulence measurements to describe flow over waves, how it is influenced by the waves and how heat and momentum fluxes are related to wind and temperature data. A number of other measurements useful especially for relating the turbulence measurements to BOMEX core experiments, were also made on FLIP during the two-week May experiment. These included humidity, sky cover, pressure, other properties of turbulent flow (such as structure functions and energy dissipations), other wave statistics, white-capping, and water currents. These were made by a

---

<sup>1</sup>Thorntwaite counters were read by University of Michigan personnel at times when the Thorntwaite system was not recording.

number of different investigators and have been, or will be described in BOMEX reports.

### III EQUIPMENT AND PROCEDURES

Wind Component Measurement. Wind components were measured with Thermo-Systems Inc. hot-film, constant temperature anemometer systems, Model 1054 B, with linearizers. Each probe (Model 1294-60) had three quartz-coated mutually perpendicular sensors 0.15 mm in diameter and 2.0 mm long. Figure 2 shows one of the probes. Each sensor is a glass rod covered with a platinum film onto which a quartz coating has been sputtered. The sensors are electrically isolated so that simultaneous measurements can be made. The orthogonal array makes it possible, with trigonometric relationships, to determine the instantaneous vector components of the wind from simultaneous measurements. The frequency response of these sensors appears to be well over 50 Hertz in the conditions under which they were used<sup>1</sup>.

In comparison to hot-wire sensors, the hot-film sensors have the following advantages:

1. Calibration stability is better because the quartz film protects the conductor from physical damage, electrical shorting and corrosion.
2. Hot-film sensors can be larger and stronger with the same electrical characteristics to maintain suitable frequency

---

<sup>1</sup>The manufacturer states that the "relative frequency response" of this element is 15,000 Hz. Relative frequency response is explained as "Response relationship between sensors when used with an 80 KC constant temperature anemometer in air at 300 ft sec<sup>-1</sup>." (Thermo-Systems Inc. Bulletin No. N16-2, page 3.)



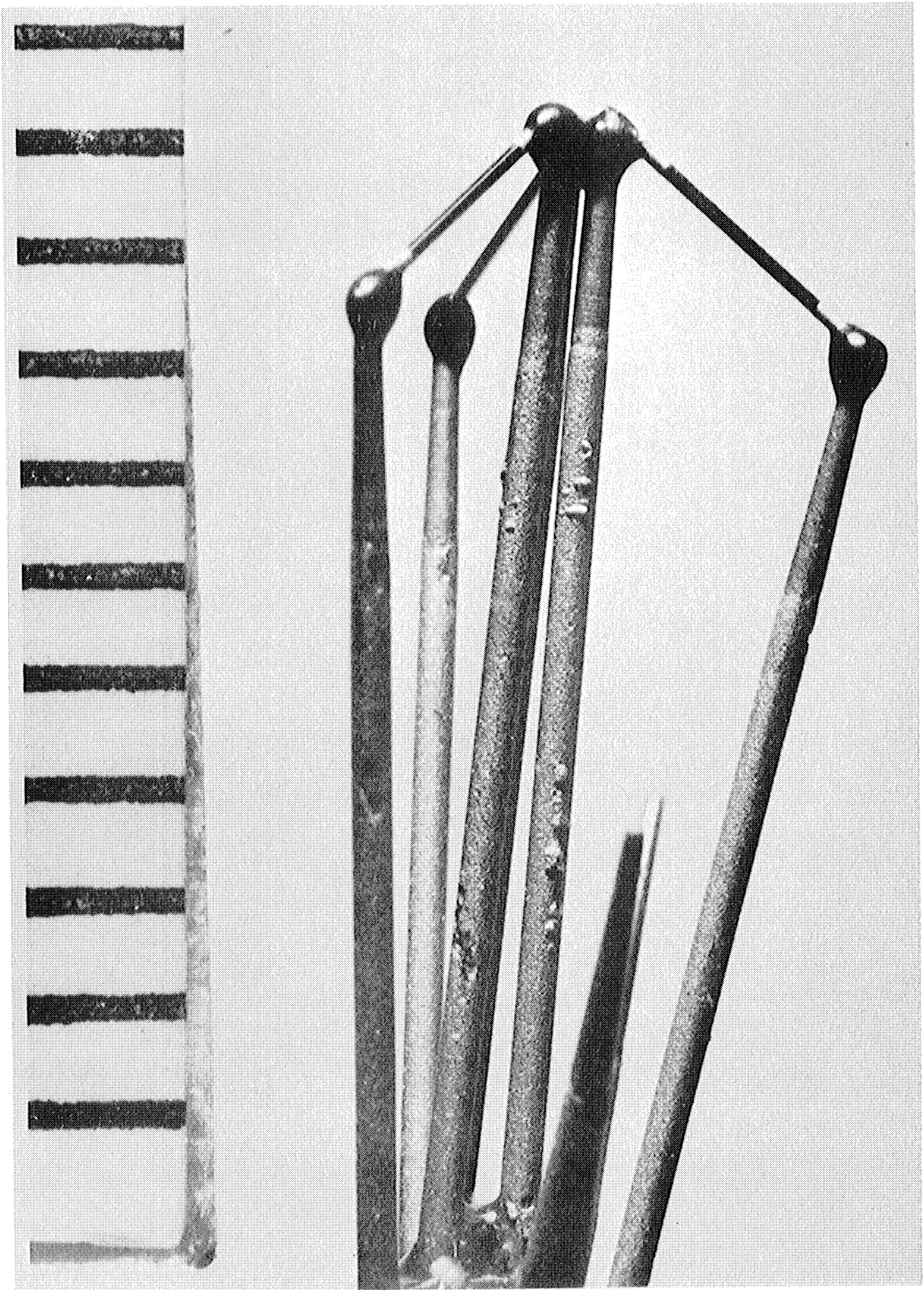


Figure 2. Three-sensor hot-film probe. A millimeter scale is shown on the left.

response.

3. Increased rigidity reduces the possibility of vibration, and hence of spurious velocity fluctuations.

The constant temperature anemometer system measures velocity by sensing the heat loss from the heated sensor to the moving air. If the air density is nearly constant and if the sensor is maintained at a constant and relatively high temperature, the heat loss is dependent almost entirely on air velocity. The sensor is part of a bridge circuit. If its resistance tends to change due to a temperature change from a change in heat loss rate (due to a change in velocity) a high gain D.C. amplifier senses the bridge off-balance and adjusts the bridge current to restore the sensor to its original temperature. The feed-back current maintains the sensor at nearly constant temperature and the corresponding voltage is a measure of the air velocity.

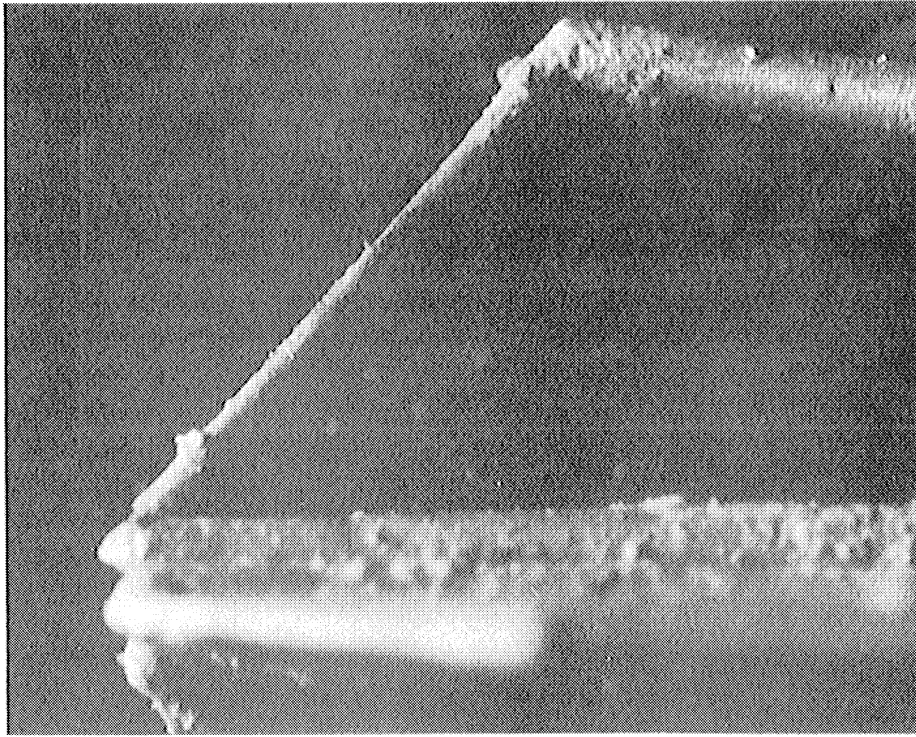
The voltage-velocity relationship is not linear so that if accurate measurement is to be made of velocity with large fluctuations it is advantageous to linearize the bridge output. The Model 1054-B anemometer systems used in this experiment had built-in linearizing circuits that provided 0 to 10 volts for a velocity range of 0 to 30 m sec<sup>-1</sup>.

The frequency response of the entire system was limited by extension leads to the sensors. Because of the mounting arrangement on FLIP it was necessary to have leads from the sensors to the electronics 40 m long. With this length of conductor between the sensor and bridge-amplifier, the system was capable of response to frequencies up to 50 Hz with no signal loss.

Individual sensors were calibrated frequently during the two week experimental period. A Thermo-Systems Inc., Model 1125, calibrator, with a compressed air flow system, was used. A previously calibrated sensor, used only for calibration, was maintained as a standard with which exposed sensors were compared in the calibrator. Flow rates were 10, 15, 20 and 30 m sec<sup>-1</sup> with the last flow rate used to set the span adjustment on the linearizer. Because some sensors had to be replaced during the experiment, the calibrations served also to evaluate the angles between the three sensors on a probe.

The photograph in Figure 3 shows a sensor (30-times magnified) after 32 hours of exposure over waves. The sensor and its needle supports appear to be partially covered with salt crystals. A calibration change in this sensor after 16 hours of exposure, during 8.75 hours of which it was in use, is shown in the graph (Figure 3). It can be seen that a 10 per cent decrease in output occurred and, following that change, the calibration apparently remained constant for another 5 hours of operation. The change in calibration may have occurred suddenly, of course, at any time between the 10th and 26th hour of exposure. In general, sensors used during any measurement period had not been exposed to the airflow for more than 8 hours or operated for more than 5 hours. The actual calibration status of sensors being used at a given time was dependent on the convenience of access to the probes.

Air Temperature Measurement. Air temperature fluctuations were measured with a Flow Corporation, Model 900-A (two-channel), anemometer system operated in a constant current mode. The tem-



Hot-film probe contaminated by salt crystals (magnification x 30) after being exposed to wind over ocean waves for 32 hours.

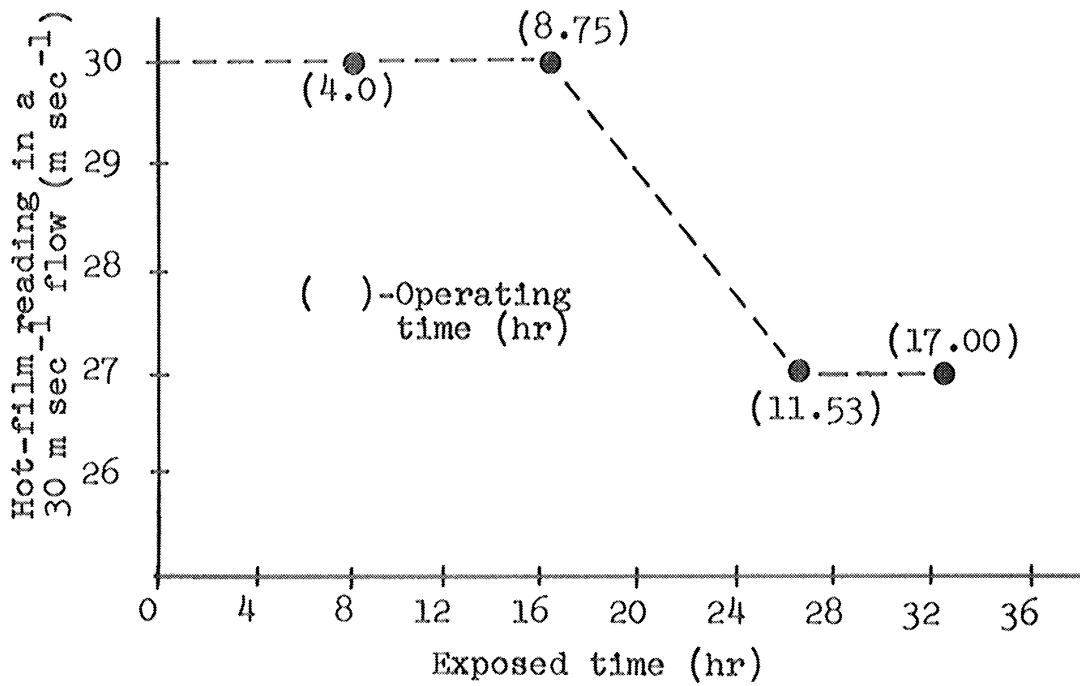


Figure 3. Hot-film sensor after use in BOMEX.

perature sensor (Flow Corporation, Model HWP-B) was a 30 ohm tungsten filament, 0.0038 mm in diameter and 5 mm long. It was operated as part of a bridge circuit with a filament current of about 2 milliamperes.

The complete system included a Flow Corporation Model 900-1 constant temperature anemometer, a Model 900-2 Monitor and Power Supply Unit and a Model 900-3 Suppressor/Filter Unit. The bridge unbalance caused by a temperature change is amplified 2500 times for the output signal. An output of 125 millivolts corresponded to about a 1°C change. Manufacturer's specifications for this system are: Frequency response from d-c to 1 KHz, resolution 0.03°C and noise level 0.33 millivolts. In a laboratory test, however, with a constant, controlled temperature and various filament resistances to simulate temperature changes, it was found that the system was capable of resolving temperature to only 0.05°C.

Calibration consisted of a determination of the output voltage for different filament resistances and reliance upon standard values for the resistance-temperature relation for tungsten.

Wave Measurement. Wave data were obtained from a resistance gauge kindly made available by Dr. R. E. Davis, Scripps Institution of Oceanography. The probe consisted of a nonconducting tube, approximately 2.5 cm in diameter, with a conducting wire wrapped spirally around it. It was positioned about 5 m inboard from the vertical mast that held the velocity and temperature sensors and was one of several used by Dr. Davis during the experiments.

Sensor Mounting Arrangement. Figure 4 shows the locations of sensors for turbulence, profile and wave measurements on the

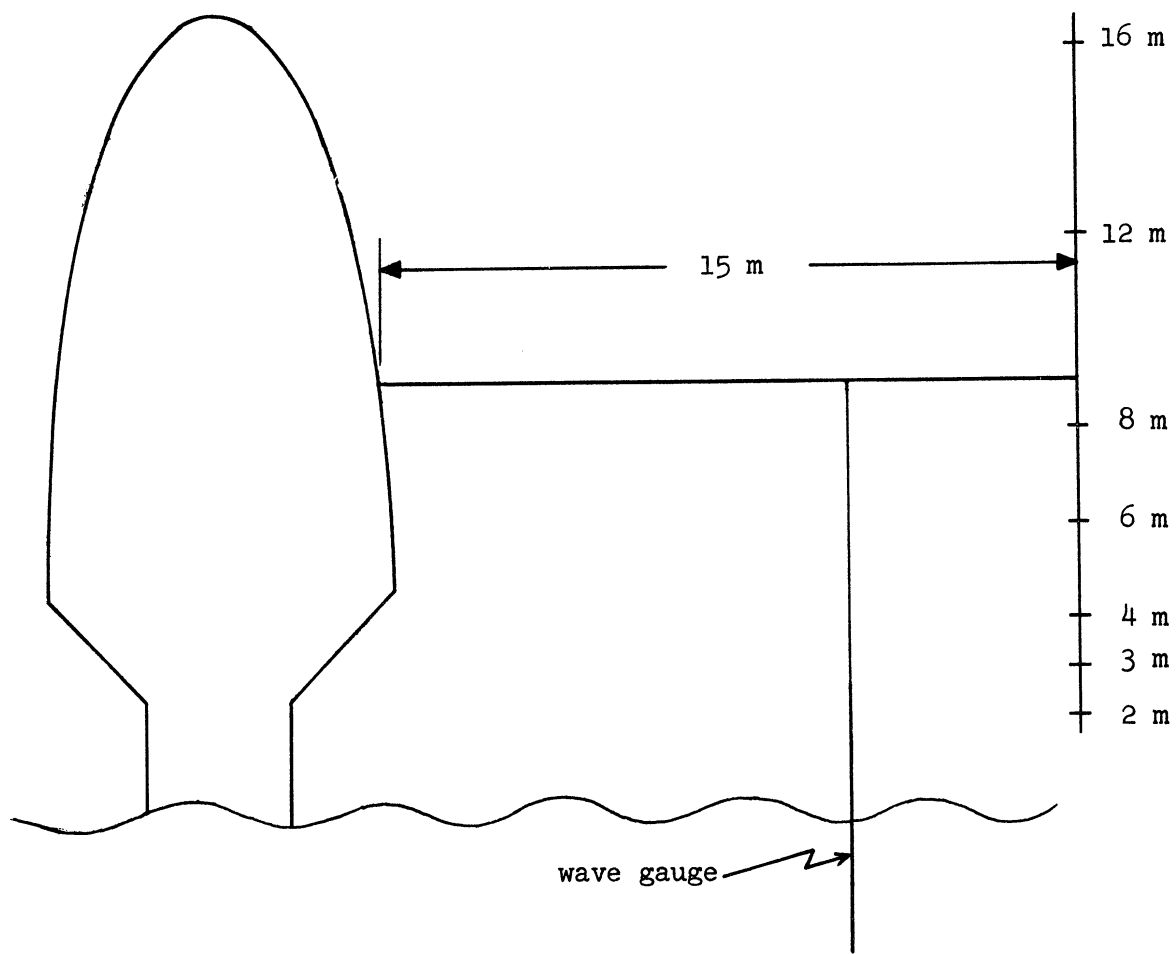


Figure 4. Sensor locations on FLIP.

vertical mast attached to FLIP. The photograph (taken on 18 May) in Figure 5 shows sensors mounted at the 2, 3, 4, 6, 8 and 10-m<sup>1</sup> levels. In this photograph, turbulence sensors are seen at the 3 and 8-m levels. All sensors were more than 1 m windward from the vertical mast and the turbulence sensors at different heights were aligned in the vertical.

As can be seen in Figure 4 the vertical mast, supported by a horizontal boom, is about 15 m from FLIP's hull. The mast was attached to a carriage that could move horizontally on the boom. In addition, the mast could be turned on a horizontal axis so that it could be brought alongside a working platform to replace and adjust sensors during the experiment.

FLIP was held by a line to a tug boat positioned downwind in order to maintain sensors properly oriented into the wind. It was estimated that the downwind drift of the vessels was never more than  $0.5 \text{ m sec}^{-1}$  and usually less than  $0.25 \text{ m sec}^{-1}$ , during the observation periods. Oscillatory motion of FLIP was measured during the experiment by Dr. R. E. Davis of Scripps Institution of Oceanography. The results of an analysis of his measurements will determine whether or not corrections for such motion will have to be applied to turbulence and wave data<sup>2</sup>.

There is a possibility that some of the wind and temperature measurements were influenced by wind field distortion due to the

---

<sup>1</sup>Sensors at the 10-m level were hot-film anemometers operated by Prof. Guy A. Franceschini of Texas A and M University.

<sup>2</sup>Physical dimensions and response of FLIP to wave motion are outlined by Bronson and Glosten (1965).



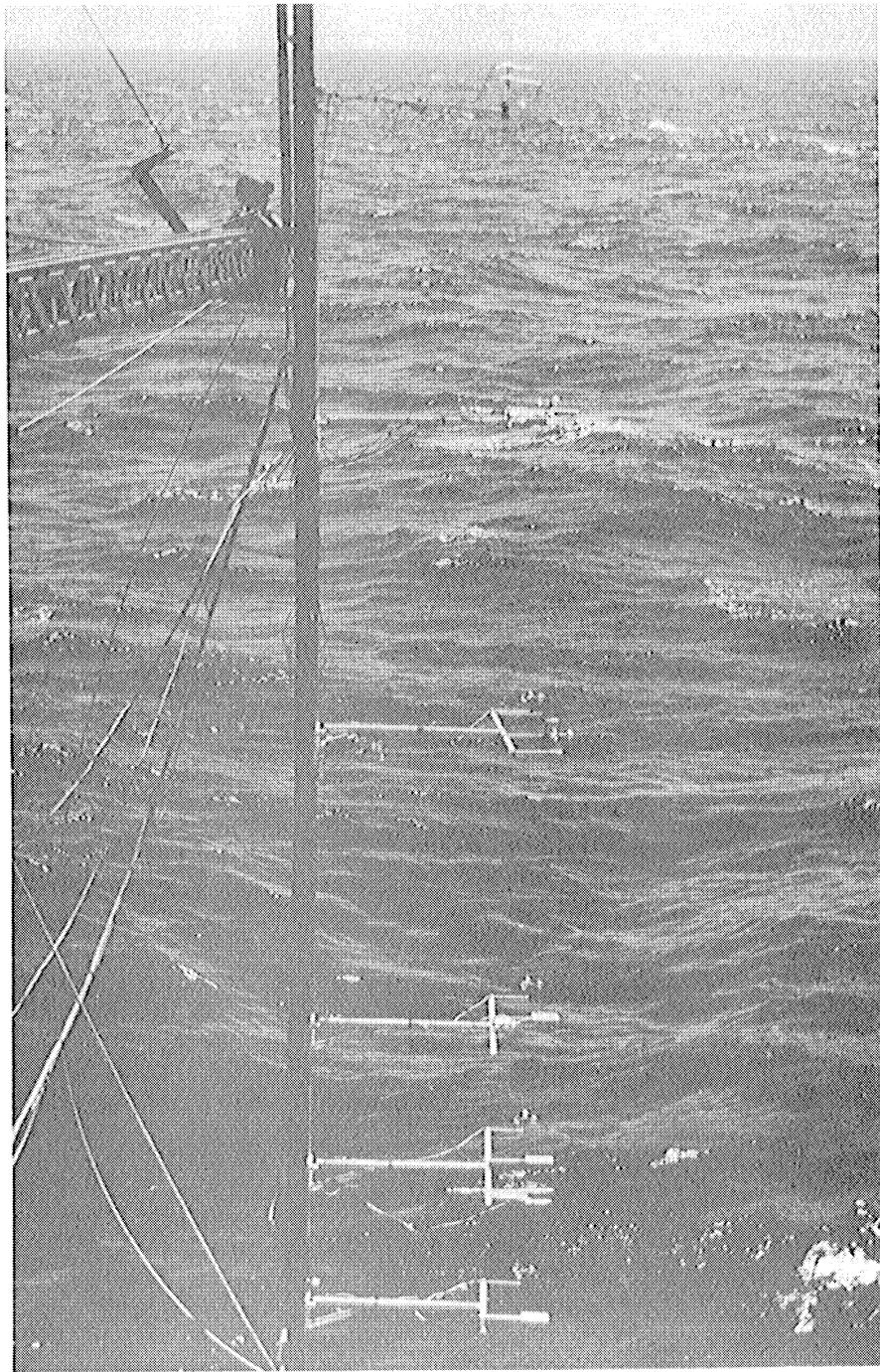


Figure 5. Sensor mounting arrangement on FLIP.



super-structure of FLIP. Mollo-Christensen (1968) in a report of wind tunnel tests of a model of the vessel suggested that measurements made within a meter of the water surface, at the position of the vertical mast, would be contaminated by distortion in the flow. The velocity measured at the top of the mast was found, in addition, to be less than about 1.5% too high. The extent of influence of any flow distortion may never be known, but it may be possible to detect any significant effects in final results of the analysis of the turbulence statistics.

Recording System. Sensor system outputs were recorded by frequency modulation on two Ampex, Model SP-300, seven channel, magnetic tape recorders with one-quarter inch magnetic tape. Before they were recorded, however, they were amplified and suppressed, with a known and constant opposing voltage, as indicated by the schematic diagram shown in Figure 6. A Tetronix dual channel oscilloscope, Type 545 B, was used to monitor simultaneously inputs and outputs of various parts of the recording system.

All recordings were made at a tape transport speed of 3-3/4 ips, making it possible, according to recorder specifications, to resolve frequencies between d-c and 625 Hz. A signal generator supplied, simultaneously, a 300 Hz sine wave to one channel of each recorder in order to synchronize the data on the separate recorders. The amplitude of the sine wave was changed at intervals to identify tape positions and to control digitizing in the data processing procedures. Such control also prevents frequency aliasing that might otherwise result from irregular tape transport both in recording and in playback.

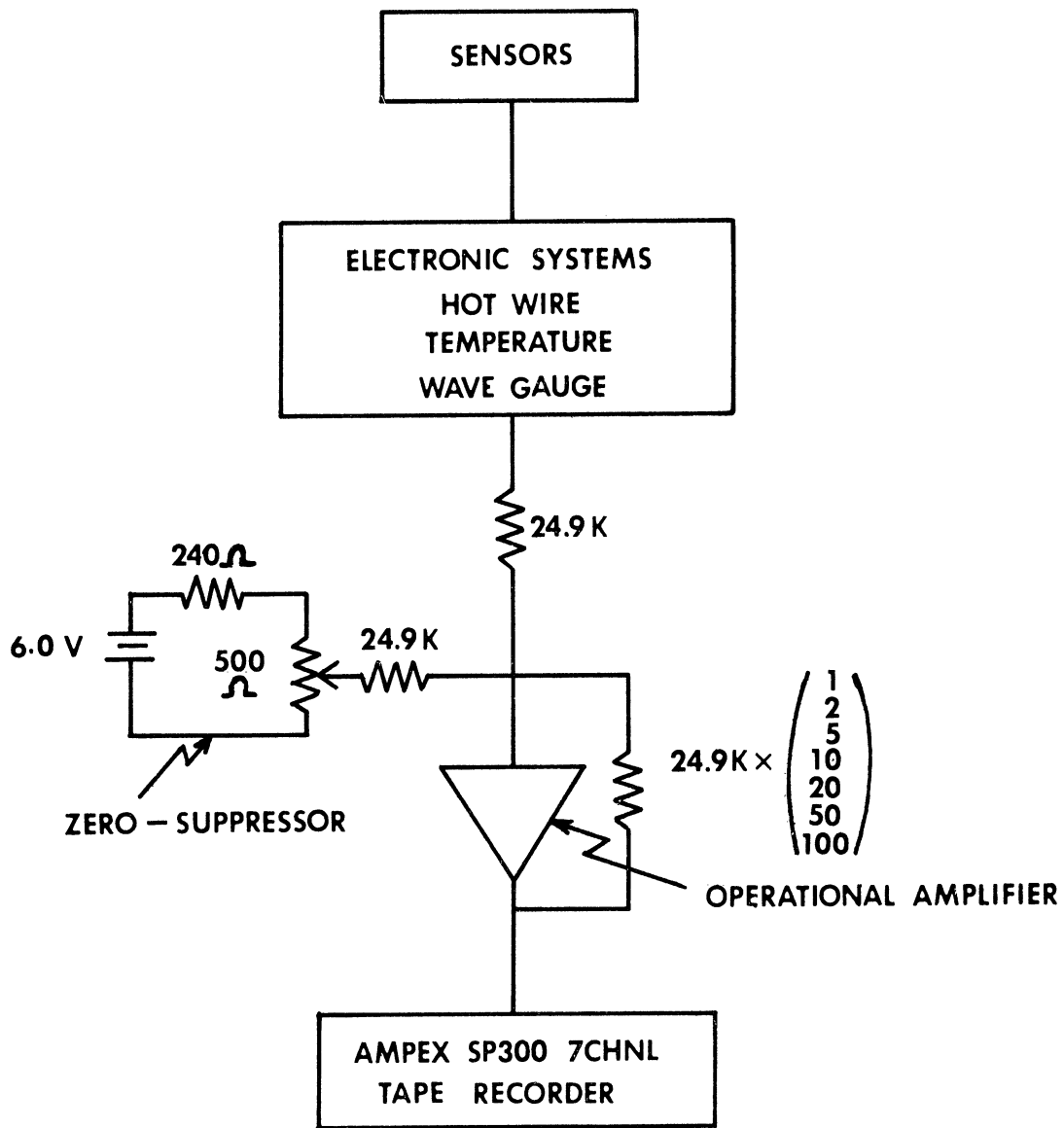


Figure 6. Schematic of recording system components.

#### IV DATA PROCESSING PROCEDURES

Descriptions of waves and turbulence in terms of probability distribution functions, joint probability distribution functions, spectrum functions and cross-spectrum functions are desired to study interaction processes. Descriptions of such functions are commonly given in terms of variances, covariances, skewnesses, coherences and other statistical parameters. The covariances for  $u'$  and  $w'$ , and for  $w'$  and  $T'$ , for example, enter the turbulence energy balance equation which is to be studied for different heights and for different wave conditions. Digital processing procedures were chosen to obtain the required statistical information from turbulence recordings.

Efficient algorithms are necessary because data consist of from 5 to 9 variables with up to 130,000 points in each time series. Fortunately all variables can be treated similarly, so one set of computer programs was sufficient. Considerable effort was involved in selecting and implementing data conditioning routines, low-pass filters and methods for evaluating the significance of results in terms of statistical confidence and physical relevance.

Figures 7 and 8 show the basic flow of the processing scheme. The analysis has been divided into two parts: (1) to obtain zero-lag statistics: means, standard deviation, skewness and kurtosis values for all variables, and covariances between all combinations of  $u'$ ,  $v'$ ,  $w'$ , and  $T'$  for 7-minute periods, and (2) to obtain smoothed and unsmoothed variance and covariance spectra,

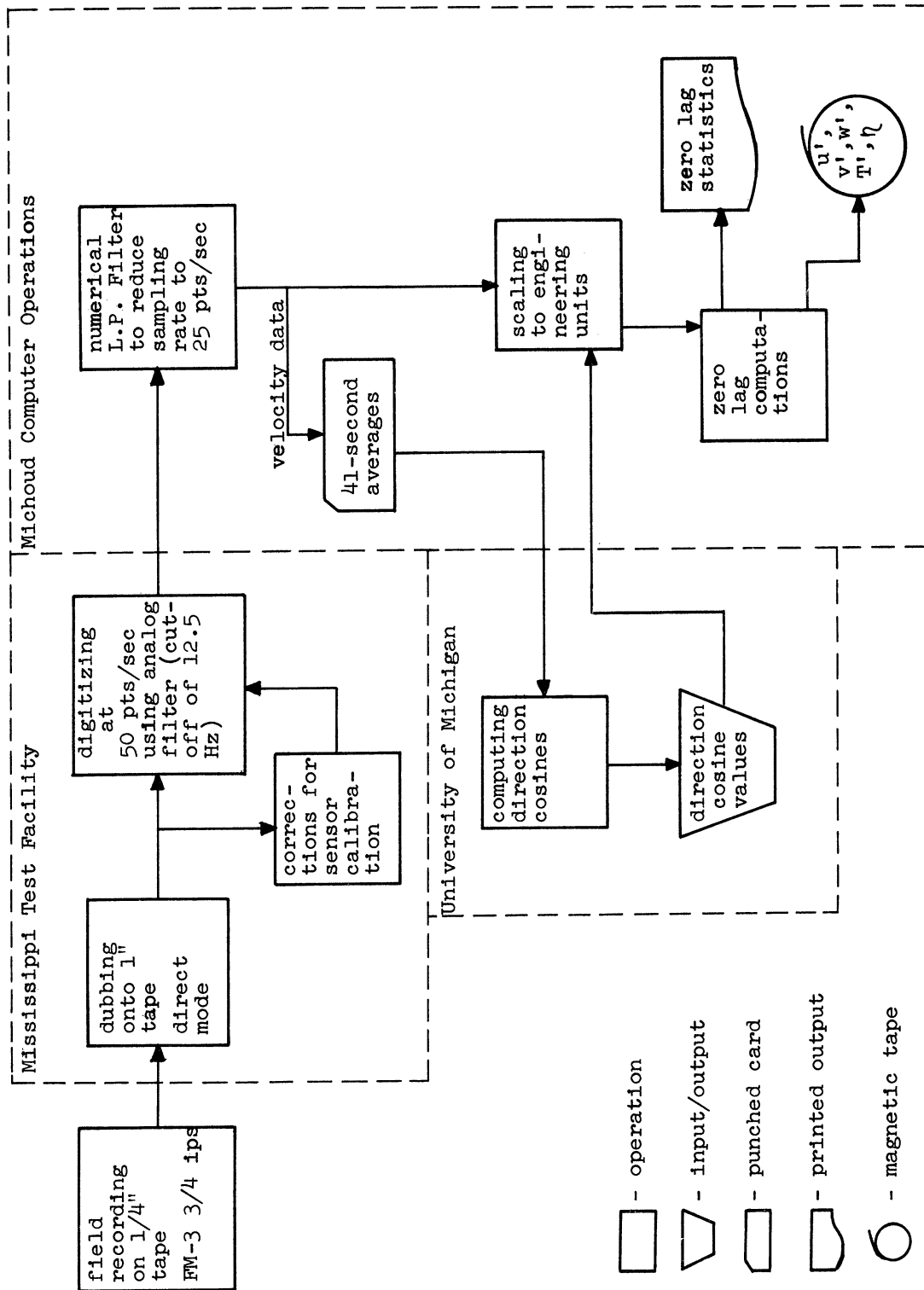


Figure 7. Data processing, stage 1.

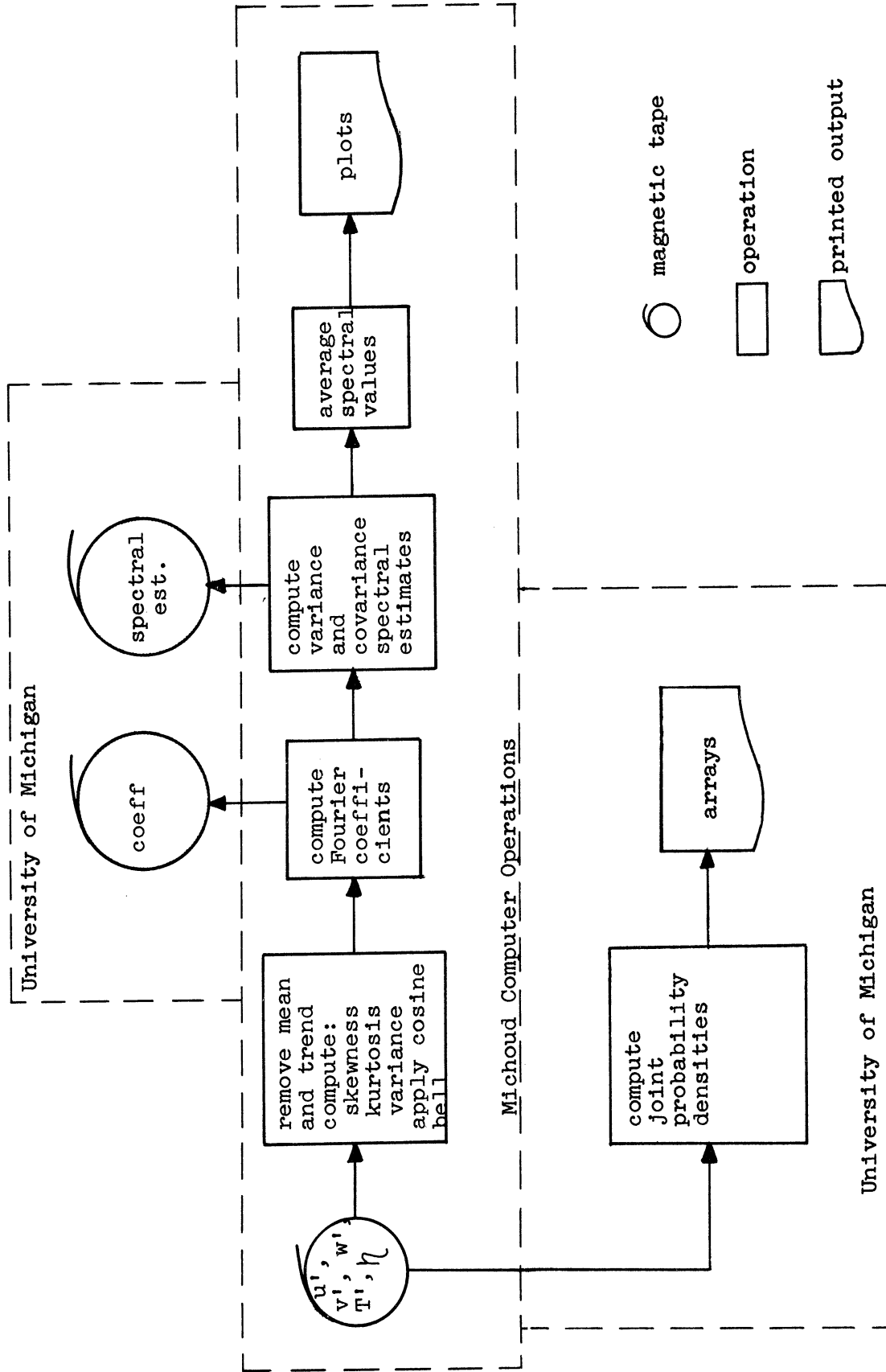


Figure 8. Data processing, stage 2.

and joint probability densities and conditional means.

As indicated in Figure 7, three different computer facilities were used in the data processing. Digitizing and initial data conditioning were conducted at the NASA Mississippi Test Facility at Bay St. Louis, Mississippi. Additional filtering and computation of zero-lag statistics and spectral data are done at the NASA Michoud Computer Operations, Slidell, Louisiana, while direction cosines for processing hot-film anemometer data and joint probability and conditional mean density data are obtained with the University of Michigan computing facilities.

Digitizing analog records. It was necessary, first, to dub (reproduce in the direct mode) the data recorded on 1/4-inch tape onto one-inch tape. The data were then digitized at 50 points per second and an analog filter was used to remove all frequencies greater than 12.5 Hz. At the same time, corrections for gain and drift were made with calibration signals recorded before each field run. The analog data ranged from -2 to +2 volts and the range of the analog-to-digital converter was -2000 to +2000 divisions. All variables recorded simultaneously in the field were digitized in parallel and identical filters were used.

Computation of zero-lag statistics. The digitized records were numerically filtered with a 5-weight inverse-transform smoothing function whose high frequency cut-off was about 7 Hz and whose terminal frequency was about 12.5 Hz. The filter was applied to every other point in each time series so that the effective sampling rate was reduced to 25 points per second.

At this stage, 41-second averages (1024 data points) were computed for hot-film anemometer data, punched onto computer cards and sent to the University of Michigan. Because of the probe's arbitrary orientation in the field, it was necessary to compute wind components relative to the mean wind from those indicated by the fixed probe. Nine direction cosines, three for each component, are determined and with these values as additional computer input, all variables are scaled to engineering units. During the process the anemometer data are converted to velocity component fluctuations by taking differences from means.

Second, third and fourth moments are then computed for consecutive 7-minute periods for each time series. In addition to serving as preliminary results, these statistics are used in the selection of data to be further processed. For example, a high kurtosis value would indicate a number of erroneous values contained in a data set. A magnetic tape containing  $u'$ ,  $v'$ ,  $w'$ ,  $T'$  and  $\eta$  records is written at this time and held for spectral and joint probability analyses.  $\eta$  is wave amplitude.

Spectral analysis. The spectral analysis begins with the removal of means and trends, and the recomputation of statistical parameters for probability distribution functions. An harmonic analysis is then performed for each time series with the Fast Fourier Transform, an algorithm due to Cooley and Tukey (1965). Spectral density estimates are then determined directly for the Fourier coefficients obtained.

Before performing the harmonic analysis, it was necessary to remove the effects of "drop-outs" and spikes that appeared in the

analog recordings. This was done by comparing the deviation of each point from the mean with the standard deviation. If a deviation was more than 4 times the standard deviation, the data point was replaced by an interpolated value (unless it occurred at the beginning or end of a record, in which case it was replaced by the mean). A comparison of the third and fourth moments before and after the conditioning showed this step to be necessary for meaningful statistics. The data were also treated with a "cosine-bell" data window (Oort and Taylor, 1969) to remove unwanted end effects resulting from the fact that the data represent finite sampling periods.

After each time series of 16,334 points is transformed, spectral estimates are obtained from 8,192 harmonics. Variance,  $\phi_{jj}(n)$ , covariance,  $\phi_{ij}(n)$ , and quadrature,  $\phi_{ij}^*(n)$ , spectral estimates are computed from the Fourier coefficients as follows:

$$\phi_{11}(n) = a_n^2 + b_n^2$$

$$\phi_{12}(n) = a_n c_n - b_n d_n$$

$$\phi_{12}^*(n) = a_n d_n + c_n b_n$$

where variable 1 =  $a + ib$   
variable 2 =  $c + id$ .

The number of points is reduced by averaging together several harmonics, or frequency bands, with a method described by Oort and Taylor (1969) and Hinich and Clay (1968). The intervals of averaging increase with frequency on a logarithmic scale. Phase lag and coherence estimates are obtained from the smoothed cospectrum and quadrature spectrum estimates.



Joint probability analysis. A joint probability density, conditional mean function computer program was written following a scheme described by Holland (1968). Three simultaneous time series form the input to the process. Means and standard deviations are computed for each series. Then for each value within a set, the deviation from the mean of its set is normalized by dividing by the set's standard deviation. For example, if  $x(i)$  = value in a set,  $\bar{x}$  = mean of all  $x(i)$ 's and  $\sigma$  = standard deviation of all  $x(i)$ 's, the program computes  $(x(i) - \bar{x})/\sigma$ . This computation is carried out for all values of each of the three variables. Two of the variables are considered jointly, while the third is called a conditional mean function.

For each pair of variables being evaluated jointly, two indices are computed representing their position in an 18 by 18 array of  $\sigma/2$  by  $\sigma/2$  joint class intervals. For example, if the first values in the two sets are 1.25 and 0.9 standard deviations from their respective means, their joint occurrence in time would be tabulated in the  $\sigma/2$  by  $\sigma/2$  cell with indices (3,2). The sums of the third variable for each cell are computed also. After all values have been analyzed, the number of joint occurrences in each cell is divided by the total number of observations, resulting in the probability per  $\sigma^2/4$ . The sums of the third variable are divided by the number of joint occurrences in each cell, giving the average deviation from the mean of the third variable corresponding to a particular probability per  $\sigma^2$  for the other two variables.

Isolines of probability per  $\sigma^2$  and of equal conditional mean functions can be constructed on the resulting print-out, which contains all essential statistical information for the relationships among three variables.

## V FIRST RESULTS

Sample results from the first computations of zero-lag statistics from wind and temperature measurements are given in Table 2. They are 4-minute averages (instead of the 7-minute averages subsequently computed for all data) for measurement heights of 8 m on May 18 and 2 m on May 19, but 6-minute averages for the 6-m data on May 19. The quantities tabulated are defined, in the table caption, in terms of the measured variables  $u'$ ,  $v'$ ,  $w'$ ,  $T'$  and  $\bar{U}$ .

Figures 9 and 10 show values of the non-dimensional ratios  $\sigma_{u/u_*}$ ,  $\sigma_{v/u_*}$ ,  $\sigma_{w/u_*}$  and  $\sigma_{T/T_*}$  in relation to the non-dimensional height  $z/L$ . Shown also in these figures are lines representing relationships found by Monin (1962) for measurements over land. The ratio  $\sigma_{w/u_*}$  appears to be consistently greater than that reported by Monin. The difference may be due to an increase in  $w'$  variance due to waves. The ratios  $\sigma_{u/u_*}$  and  $\sigma_{v/u_*}$  exhibit considerable scatter but the  $\sigma_{T/T_*}$  values show a general agreement with Monin's relationship.

Results of spectral analysis of simultaneous measurements of velocity component fluctuations at the 6-m level and of waves for 19 May 0308-0320 GMT (Period I) and 0945-1000 GMT (Period II) are shown in Figure 11. The average wind speed at 6 m was about 10  $\text{m sec}^{-1}$  for each period. Wave amplitudes corresponding to the wave-spectrum peaks for Period I, however, were three times greater than those for Period II. They were 3 m and 1 m for Periods I and II, respectively. The corresponding critical levels for both

Table 2

## Sample Turbulence Statistics

date (May 1969)	time(GMT)	Z	$\bar{U}$	$u_*$	$\sigma u/u_*$	$\sigma v/u_*$	$\sigma w/u_*$	$\sigma T/T_*$	$z/L$
18	0230-0234	8	789	23.8	2.60	3.50	.82		.014
	0234-0238	8	795	20.8	2.94	3.50	.93	1.24	-.065
	0238-0242	8	827	20.0	2.85	2.80	.94	1.31	-.057
	0242-0246	8	820	28.3	3.42	2.81	.83	1.26	-.044
	0246-0250	8	834	24.0	2.47	2.81	.91	1.39	-.045
	0250-0254	8	781	20.8	3.20	2.99	.97	1.07	-.074
19	0308-0312	2	989	44.3	2.30	1.54	.66	-2.71	.0028
	0312-0316	2	1007	41.2	2.37	1.78	.67	-2.66	.0054
	0316-0320	2	961	45.8	2.27	1.60	.67	-2.20	.0027
	0320-0324	2	946	36.8	2.19	1.68	.70	-1.90	.0058
	0324-0328	2	949	37.7	2.11	2.51	.80	-1.27	.0052
	0328-0330	2	957	49.5	2.08	1.80	.69	-4.12	.0019
	0332-0336	2	1003	39.7	2.10	1.77	.80	-1.97	.0054
	0336-0340	2	984	41.1	2.10	2.13	.76	-1.42	.0066
	0340-0344	2	984	41.8	2.15	2.03	.79	-1.33	.0084
	0344-0348	2	965	41.9	2.12	1.45	.66	-1.49	.0070
	0314-0320	6	1068	19.3	4.68	3.50	.79	-2.57	.020
	0945-0951	6	1053	23.9	3.74	2.67	.89	-1.57	.027
	0951-0957	6	1025	24.4	3.77	3.22	.91	-1.27	.032

Z = height of measurement, m.

$\bar{U}$  = average horizontal wind speed, cm sec<sup>-1</sup>, at height z.

$u_* = (\overline{u'w'})^{\frac{1}{2}}$ , cm sec<sup>-1</sup>.

$\sigma_i$  = standard deviation of variable i.

$T_* = \overline{w'T'}/k u_*$ , deg C.

k = von Karman number

$L = u_*^3 / (g/T)(\overline{w'T'})$ , cm.

g = acceleration due to gravity, cm sec<sup>-2</sup>.

T = absolute temperature, deg.

z = height of measurement, cm.

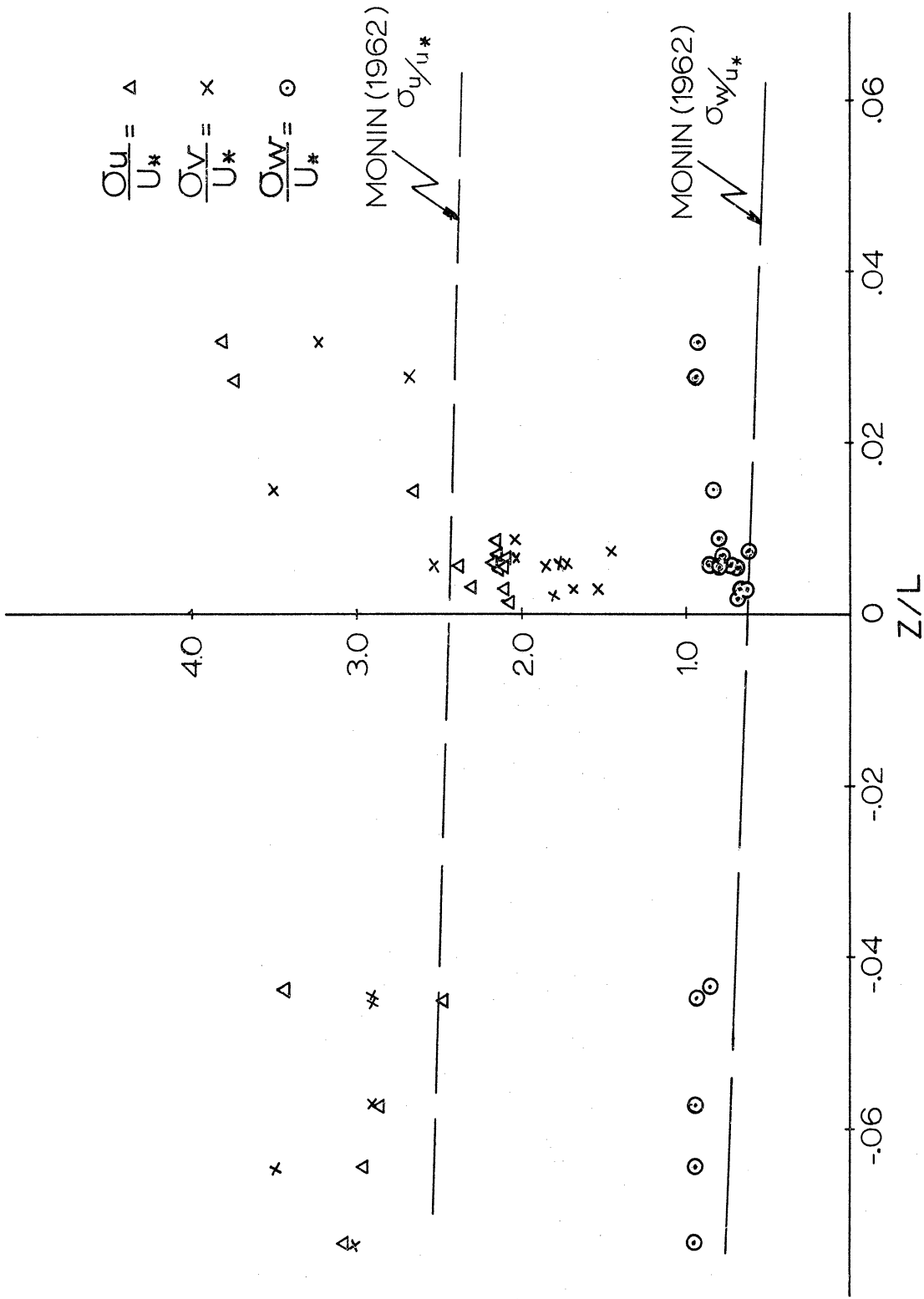


Figure 9. Non-dimensional ratios  $\sigma_u/u_*$ ,  $\sigma_v/u_*$ , and  $\sigma_w/u_*$  in relation to  $z/L$ .

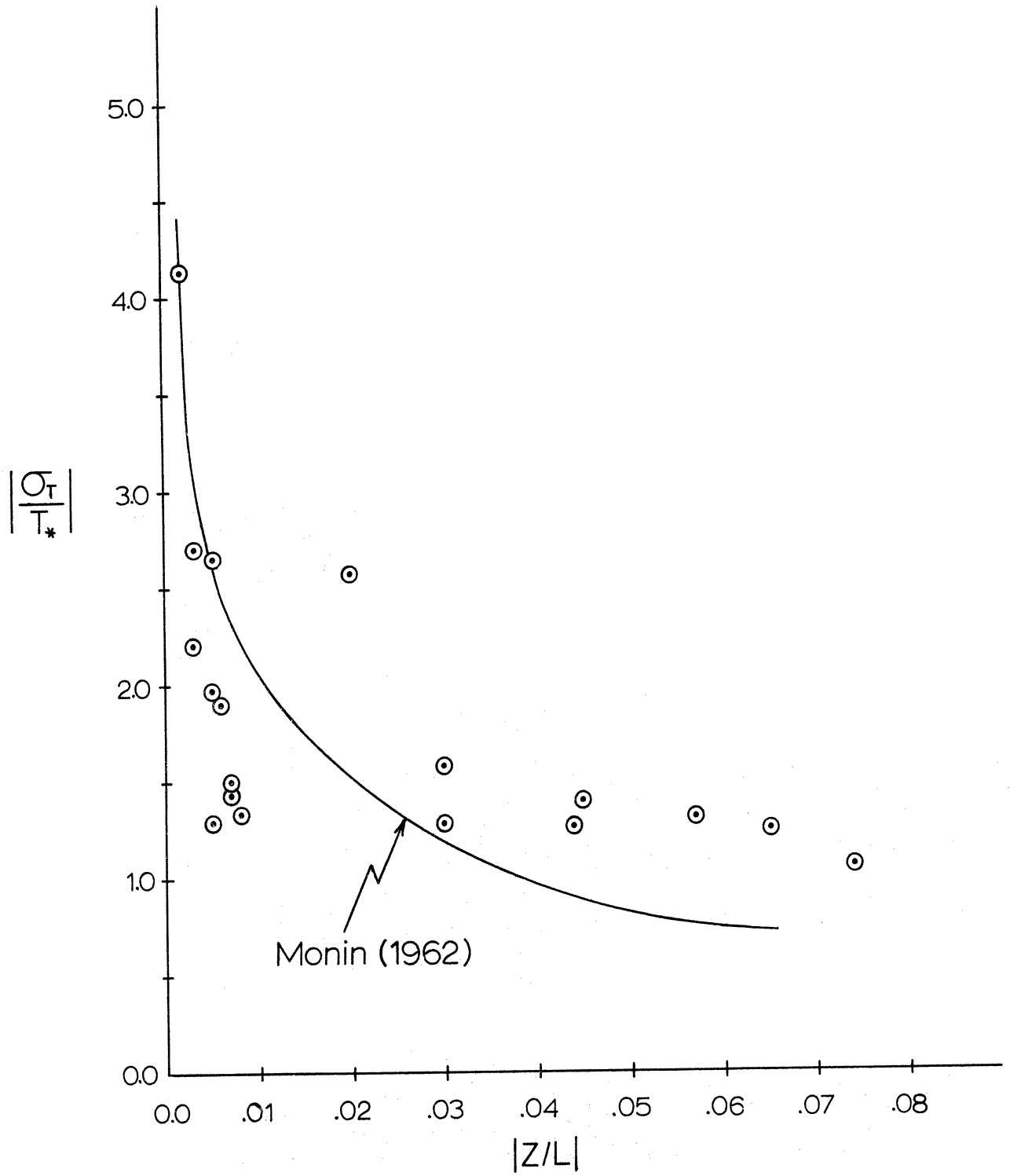


Figure 10. Non-dimensional ratio  $\sigma_T/T_*$  in relation to  $z/L$ .

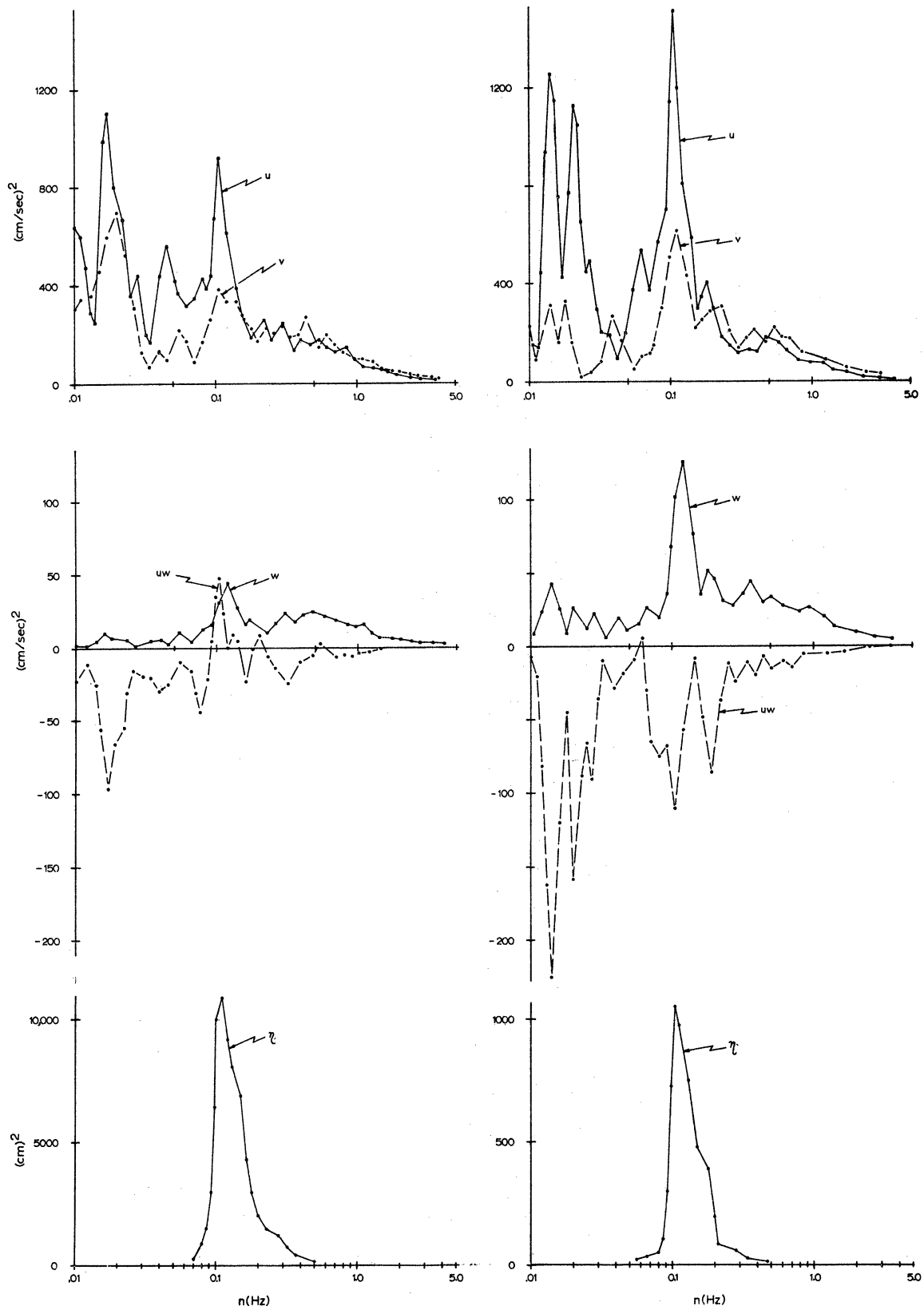


Figure 11. Spectral results for 19 May 1969.  
 Left side: Period I (0308-0320 GMT)  
 Right side: Period II (0945-1000 GMT)  
 $\eta$  - wave spectrum

periods were about 10 m.

Relatively large values of spectral density at the frequency of the wave-spectrum peaks are prominent features of the velocity spectra. There is a significant difference, however, between the  $\overline{u'w'}$  cospectra for the two periods. In Period I there are positive  $\overline{u'w'}$  values (i.e., upward transport of u momentum) at the frequencies of the wave spectrum peak while at comparable frequencies in Period II there appear to be increased negative values of the cospectrum (i.e., enhanced downward transport of u momentum). These results are similar to those reported by Davidson (1970) for measurements from a fixed platform in Lake Michigan in similar conditions. From the Lake Michigan data he found that wave height is a significant factor for determining the sign of the cospectrum of  $\overline{u'w'}$  near the wave spectrum peak.

Figure 12 shows, for the frequency of the wave-spectrum peaks, phase relations among wind velocity components u and w and assumed particle motion at the water surface. Although both sets of wind data were obtained at a height of 6 m above mean water level (MWL), they are scaled in Figure 12 according to values of Z/H, where Z is measurement height and H is dominant wave height. Period II, then, comprises the upper third of Figure 12 and Period I the middle third. In this non-dimensional height scale, it can be seen that the u and w components shift with height in opposite senses. For Period I, when the measurement height is only twice the wave height, it is evident that the maximum in the w component is nearly in phase with that of the water surface. It shifts nearly 30 degrees back toward the wave crest at a height corresponding to 6 times



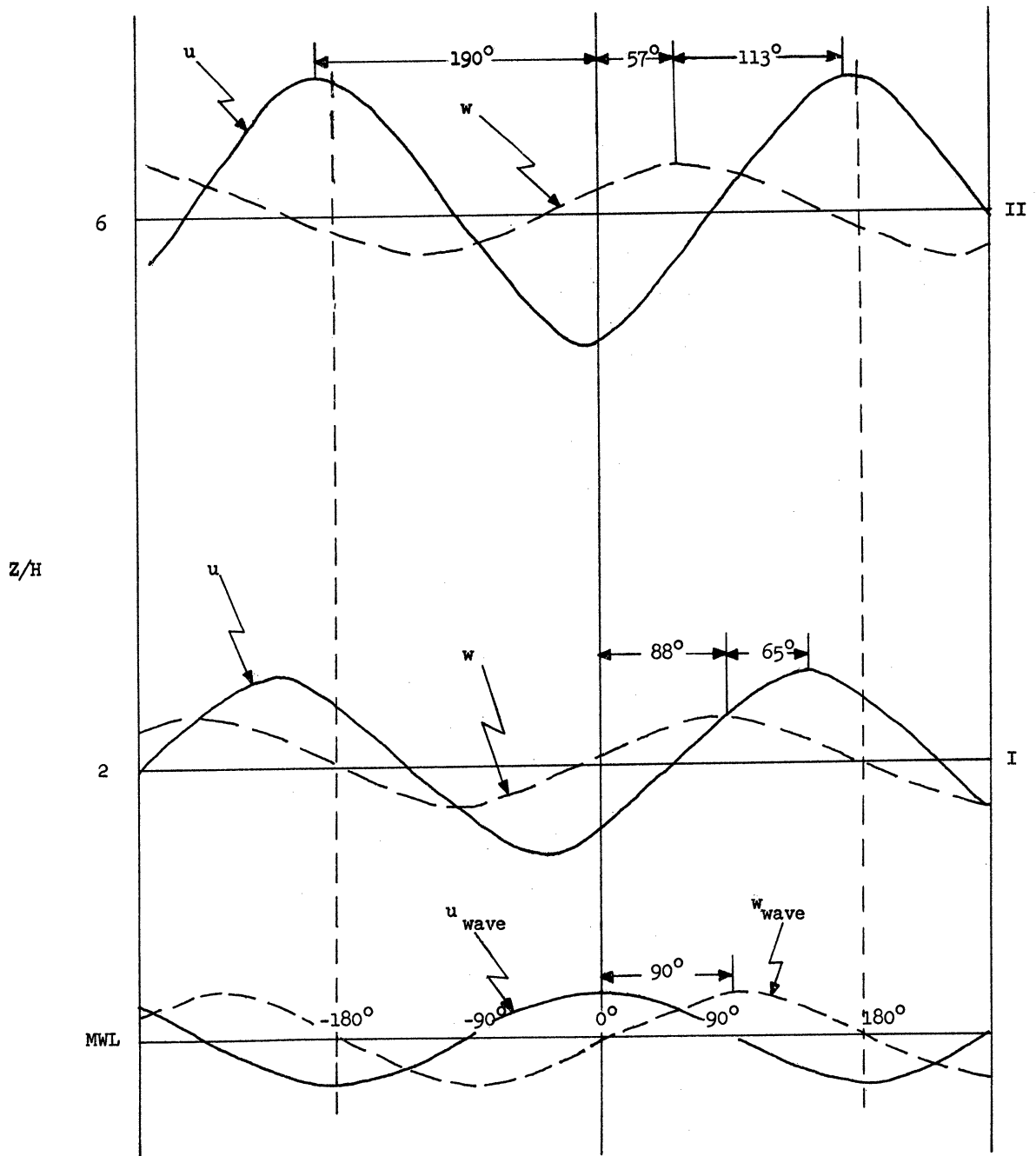


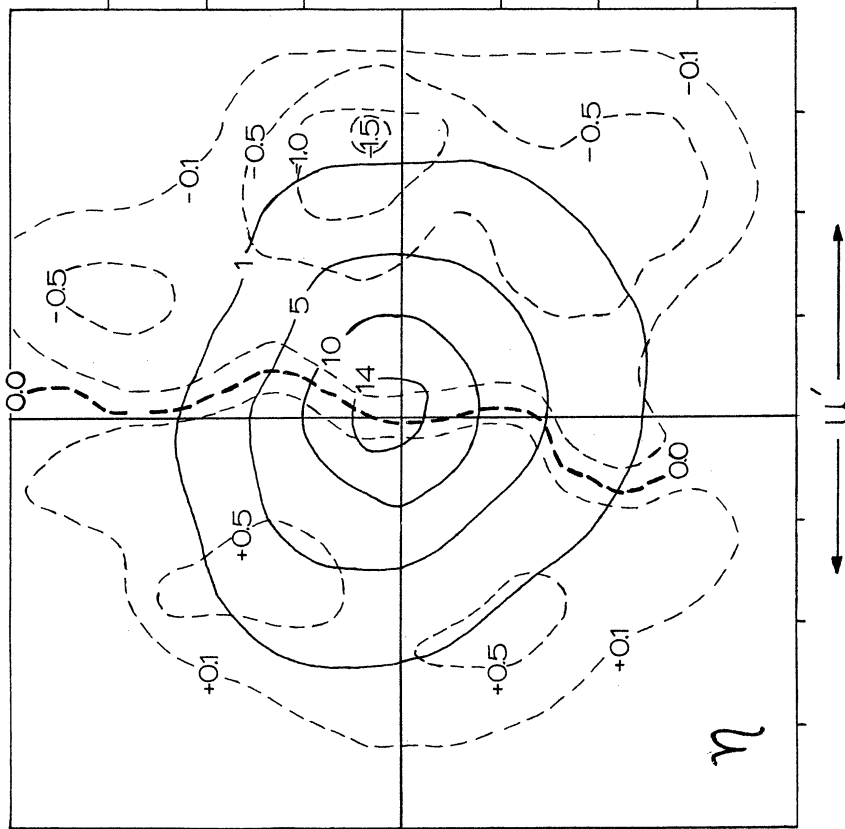
Figure 12.

Phase relationships among velocity components and components of dominant surface wave, 19 May 1969 for  
 Period I (0308-0320 GMT) and  
 Period II (0945-1000 GMT)

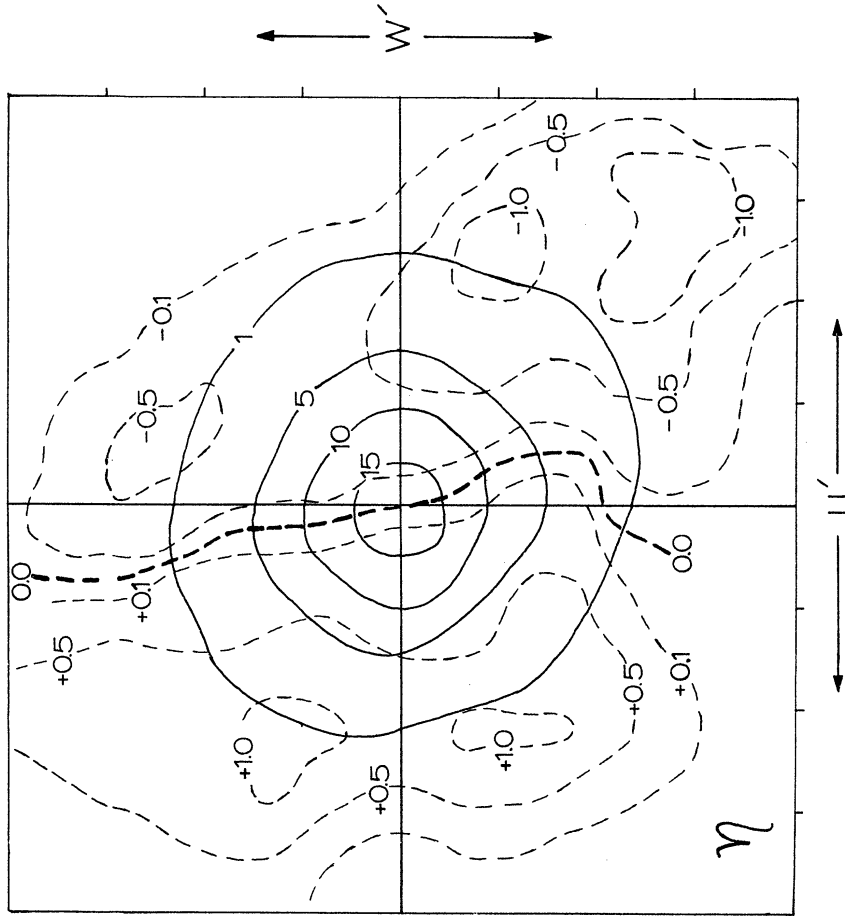
the wave height (Period II). The phase of the u component, on the other hand, shifts from 153 degrees in advance of the surface particle to 170 degrees in advance for the same non-dimensional height interval. The results may be interpreted as evidence of wave influence on the air flow over them.

Joint probability density, conditional mean function (JPDCMF) results for the same two measurement periods are shown in Figure 13. Unlike the phase relationships in Figure 12, where (for simplicity) sinusoidal curves were assumed, the JPDCMF results are based on real-time occurrences of relationships among variables. In Figure 13, the solid lines represent isolines of probability per  $\sigma^2$  for  $u'$  and  $w'$ , while the dashed lines represent average deviations from the mean for  $\eta$  (water surface displacement from MWL). In both periods large positive values of  $u'$  are associated with values of negative  $\eta$  (wave trough), and large negative values of  $u'$  occur with values of positive  $\eta$  (wave crest). Large positive and negative values of  $w'$  are associated with values of 0.0 for  $\eta$  (wave nodes). The results agree with those shown in Figure 12.

All data reported here should be regarded only as illustrative of some of the information obtainable from the turbulence measurements made from FLIP during BOMEX by University of Michigan personnel. As noted above, it is possible that the hot-film anemometer data will have to be corrected because of FLIP motions and, in addition, final results will be reported with longer averaging times.



Period I (0308-0320 GMT)  $\sigma_u = .36 \text{ m sec}^{-1}$   
 $\sigma_w = .08 \text{ m sec}^{-1}$   $\sigma_\eta = 1.0 \text{ m}$



Period II (0945-1000 GMT)  $\sigma_u = .38 \text{ m sec}^{-1}$   
 $\sigma_w = .11 \text{ m sec}^{-1}$   $\sigma_\eta = .34 \text{ m}$

Figure 13. Joint probability distributions among velocity components and dominant surface wave, 19 May 1969.

## REFERENCES

- Bronson, E.D. and L.R. Glosten, 1965: FLIP, Floating Instrument Platform. SIO Reference 65-12, ONR Contract Nonr 2216(05), Scripps Institute of Oceanography, San Diego, Cal., 21 pp.
- Cooley, J.W. and J.W. Tukey, 1965: Algorithm for the Machine Calculations of Complex Fourier Series. Math. of Comp., 19(90), 297-301.
- Davidson, K.L., 1970: An Investigation of the Influence of Water Waves on the Adjacent Airflow. ORA Report 08849-2-T, ONR Contract N00014-67-A-0181-0005, Dept. of Meteor. and Ocean., University of Michigan, 259 pp.
- Harris, D.L., 1966: The Wave Driven Wind. J. Atmos. Sci., 23(6), 688-693.
- Hinich, M.J. and Clay, C.S., 1968: The Application of the Discrete Fourier Transform in the Estimation of Power Spectra, Coherence, and Bispectra of Geophysical Data. Rev. Geophys., 6(3), 347-363.
- Holland, J.Z., 1968: An Application of Some Statistical Techniques to the Study of Eddy Structure. TID-24585, U.S. Atomic Energy Commission, Washington, D.C., 378 pp.
- Karaki, S. and E.Y. Hsu, 1968: An Experimental Investigation of the Structure of a Turbulent Wind over Water Waves. Technical Report No. 68, Department of Civil Engineering, Stanford Univ., 100 pp.
- Kitaygorodskiy, S.A., 1969: Small Scale Atmosphere-ocean Interactions. IZV. Atmospheric and Oceanic Physics, Academy of Sciences, USSR, 5(11), Translated by K. Syers, 641-649.
- Miles, J.W., 1957: On the Generation of Surface Waves by Shear Flows. J. Fluid Mech., 3(2), 185-204.
- Miles, J.W., 1959: On the Generation of Surface Waves by Shear Flows. J. Fluid Mech., 6(4), 568-582.
- Mollo-Christensen, E., 1968: Wind Tunnel Test of the Superstructure of the R/V Flip for Assessment of Wind Field Distortion. Report 68-2, ONR Contract NR 083-236, Fluid Dynamics Laboratory, Massachusetts Institute of Technology, 31 pp.
- Monin, A.S., 1962: Empirical Data on Turbulence in the Surface Layer of the Atmosphere. J. Geophys. Res., 67(8), 3103-3111.
- Oort, A.H. and A. Taylor, 1969: On the Kinetic Energy Spectrum near the Ground. Mon. Wea. Review, 97(9), 623-636.

- Phillips, O.M., 1966: The Dynamics of the Upper Ocean. Cambridge Press, Cambridge, England, 261 pp.
- Shemdin, O.H., 1969: Instantaneous Velocity and Pressure Measurements above Propagating Waves. Technical Report No. 4, Dept. of Coastal and Oceanographic Engineering, College of Engineering, University of Florida, 104 pp.
- Stewart, R.H. II, 1968: Laboratory Studies of the Velocity Field over Deep-Water Waves. Ph.D. dissertation, Dept. of Oceanography, Univ. of California, San Diego, (unpublished manuscript), 161 pp.
- Superior, W.J., 1969: BOMEX Flux and Profile Measurements from FLIP. Final Report, Naval Oceanographic Office Contract N62306-69-C-0186, C. W. Thornthwaite Associates, Laboratory of Climatology, Elmer, N. J., 32 pp.
- Yefimov, V.V. and A.A. Sizov, 1969: Experimental Study of the Field of Wind Velocity over Waves, IZV. Atmospheric and Oceanic Sciences, Academy of Sciences, USSR, 5(9), Translated by A. Peiperl, 530-537.

